International Journal of Control and Automation
Vol.7, No.2 (2014), pp.405-416
http://dx.doi.org/10.14257/ijca.2014.7.2.36

Modeling and Experimental Investigation of the Flow Velocity Field in the Grinding Zone

Dongzhou Jia[1], Changhe Li[1*] and Runze Li[2]

[1]*School of Mechanical Engineering, Qingdao Technological University, 266033 China, E-mail: sy_lichanghe@163.com*
[2]*School of Life Sciences and Technology, Huazhong University of Science and Technology, 430074 China*

**Corresponding author: Li C.H. E-mail: sy_lichanghe@163.com*

Abstract

In the grinding process, grinding fluid is delivered for the purposes of chip flushing, cooling, lubrication and chemical protection of work surface. Lubrication and cooling are the most important roles provided by a grinding fluid. Hence, the conventional method of flood delivering coolant fluid by a nozzle achieves high process performance. However, the flow velocity field can be generated ahead of the grinding zone due to the wedge effect between wheel peripheral surface and workpiece surface. According to Navier-Stokes equation and equation of continuity for fluid flow, the mathematical model of the velocity field in the wheel/workpiece wedge-shaped zone was established and simulated. Findings presented that the flow velocity increased as the velocity of the grinding wheel increased. At the direction of wheel width, the distribution patterns of the flow velocity were the same, expect the rising at the verge of the wheel. In addition, the experiment research on the velocity field in the wheel/workpiece wedge-shaped zone was also conducted. Findings demonstrated that the established model was consistent with the experimental results and the theoretical model effectively protected the distribution of the velocity field in the prediction contact zone.

Keywords: *Grinding wheel, Wedge-shaped zone, Velocity field ; Pressure*

1. Introduction

Grinding processes are techniques employed widely as a finishing. However in grinding process, high grinding zone temperature may lead to thermal damage to the work surface, induces micro-cracks and tensile residual stresses at the ground surfaces, which deteriorate surface quality and integrality of the ground surface. This damage can be reduced by the application of a flood delivery grinding fluid that removes the heat created by the workpiece interaction and lubricates the two surfaces in order to decrease the amount of friction. Hence, numbers of investigations have been mainly focused on the fluid delivery methods that make large volumetric flow-rate into the grinding zone in order to overcome boundary layer of air [1-6]. However, due to the wedge effect between wheel and work surface, the flow velocity field is generated considerably in the flood delivery grinding process. Moreover, conventional methods of flood delivering coolant fluid via a shoe nozzle tangential to the wheel are not believed to fully penetrate this boundary layer of air. Consequently, the majority of grinding fluid is deflected away from the grinding zone [7-10]. Therefore, the flood delivery of a grinding fluid not only that increase hydrodynamic lift force, result in reduce the depth of cutting [11-12], and increase grinding wheel spindle distortion, but also that increase high

ISSN: 2005-4297 IJCA

disposal costs in production, create several techno-environmental problems, biological problems, and soil contamination.

The velocity field of grinding fluid across the wedge-shaped zone has been investigated both theoretically and experimentally. Ganesan *et al.* measured the flow velocity field by experimentally. Results indicated that the fluid velocity field rises progressively with wheel speed. Cutting depth and feed rate had comparatively little influence [13].Ganesan measured normal hydrodynamic force for various gap thicknesses between the wheel and the workpiece. Hydrodynamic forces were analyzed at the wedge-shaped zone by applying classical hydrodynamic theory with laminar flow [14]. Klocke *et al.* calculated the hydrodynamic pressure in the converging gap between the wheel and the workpiece using the Reynolds equation. The gap size between grinding wheel and workpiece was measured using a mechanical-inductive transducer with a diamond probe [15-17]. Brinksmeier and Minke investigated the influence of fluid in high-speed surface grinding with electroplated CBN wheels. High normal force was measured, caused by the fluid contact pressure. The normal force increased with wheel speed and delivered flow rate [18-20]. Frank *et al.* pointed out that hydrodynamic lift force is remarkably high in the overall grinding resistance, and suggested that a grooved wheel was effective to release the pressure generation [21-22]. Furutani *et al.* suggested a new in-process method to monitor not only the topographical grinding wheel conditions such as loading or dulling but also the real displacement of wheel spindle caused by the overall grinding resistance [23-24]. Moreover, some research groups tried new polishing techniques by adopting NC control of polishing wheel, which provides not only the fluid velocity field but also high speed particle motion generated by both fluid speed and centrifugal force in the near contact zone [25-28].

Though a number of investigations mentioned above have shown that the fluid velocity field and hydrodynamic pressure in grinding zone are of great importance in respect to many aspects of grinding process [29]. A comprehensive model that could predict grinding fluid hydrodynamic pressure and the velocity field has not yet emerged. The goal of this project is investigate the fluid velocity field modeling in conventional flood delivery grinding by theoretically and experimentally so as to find the quantitative relationship between the fluid velocity field and grinding conditions.

2. Modeling of the Velocity Field

To study on the flow field in the contact zone, the following simplifications and assumptions were conducted:

The wheel surface was smooth (considered based on the average smooth surface of the abrasive particles); the impact of temperature and pressure on the fluid viscosity were neglected and the fluid pressure along the film thickness remained unchanged; the fluid was incompressible Newtonian fluid. The flow of the fluid in the clearance was laminar flow, and the inertial effect in the flow was not considered.

Based on the above assumptions, the Navier-Stokes equation can be simplified as:

$$\frac{\partial p}{\partial x} = \mu \frac{\partial^2 u_f}{\partial z^2} \tag{1}$$

$$\frac{\partial p}{\partial y} = \mu \frac{\partial^2 v_f}{\partial z^2} \tag{2}$$

$$\frac{\partial p}{\partial z} = 0 \tag{3}$$

Where u_f and v_f stand for the fluid velocity along x and y; p is the dynamic pressure of the fluid in the wedge-shaped area; μ is the dynamic viscosity.

Eq.(1) achieves two integrals of z, and the boundary conditions were taken as: when $z = 0$, $u_f = 0$; when $z = h$, $u_f = v_s$, we can obtain:

$$u_f = \frac{1}{2\mu}\frac{\partial p}{\partial x} z(z-h) + \frac{v_s}{h} z \tag{4}$$

Where v_s is the peripheral velocity of the grinding wheel, h stands for the clearance between the wheel and the workpiece:

$$h(x) = h_0(1 + \frac{x^2}{2Rh_0}) \tag{5}$$

Where h_0 is minimum interval between the wheel and the workpiece, and R is the radius of the grinding wheel.

In the same way, Eq.(2) achieves two integrals of z, and the boundary conditions were taken as: when $z = 0$, $v_f = 0$; when $z = h$, $v_f = 0$, we can obtain:

$$v_f = \frac{1}{2\mu}\frac{\partial p}{\partial y} z(z-h) \tag{6}$$

p in Eq.(4) and (6) is the dynamic pressure formed in the wedge-shaped area, that is:

$$\frac{\partial}{\partial x}(\frac{h^3}{12\mu}\frac{\partial p}{\partial x} - \frac{h}{2}U) + \frac{\partial}{\partial y}(\frac{h^3}{12\mu}\frac{\partial p}{\partial y}) = 0 \tag{7}$$

Dynamic pressure boundary condition can be shown in Fig.1. The boundary conditions were defined as:

$$p\big|_{x=a} = 0, -\frac{b}{2} \le y \le \frac{b}{2}$$

$$p\big|_{y=\pm b/2} = 0, a \le x \le c$$

At the outlet, Reynolds boundary conditions were used: $\left.\frac{\partial p}{\partial x}\right|_{x=c} = p\big|_{x=c} = 0, -\frac{b}{2} \le y \le \frac{b}{2}$

Where b stands for the wheel width; a is the length of the inlet in the definite contact zone; c is the length of the outlet of the definite contact zone.

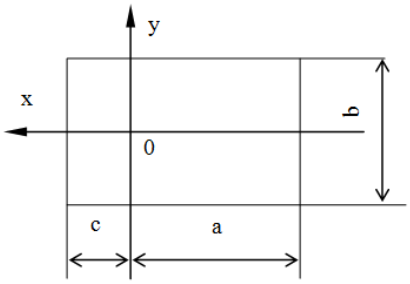

Figure 1. Dynamic pressure boundary condition

3. Model simulation

3.1 Changes of the flow velocity along the X direction

The grinding wheel has the diameter of 200 mm and the width of 30mm, the dynamic viscosity of the grinding fluid is 0.05Pa s, and the minimum interval between grinding wheel and workpiece is h_0 = 50 μm. With the above conditions remaining fixed, only the peripheral velocity of the grinding wheel was changed. The variation trend of the fluid velocity in the contact area in direction *x* was calculated, and in calculation, the peripheral velocities (v_s) of the grinding wheel were 50 m/s, 80 m/s, 120 m/s and 160 m/s.

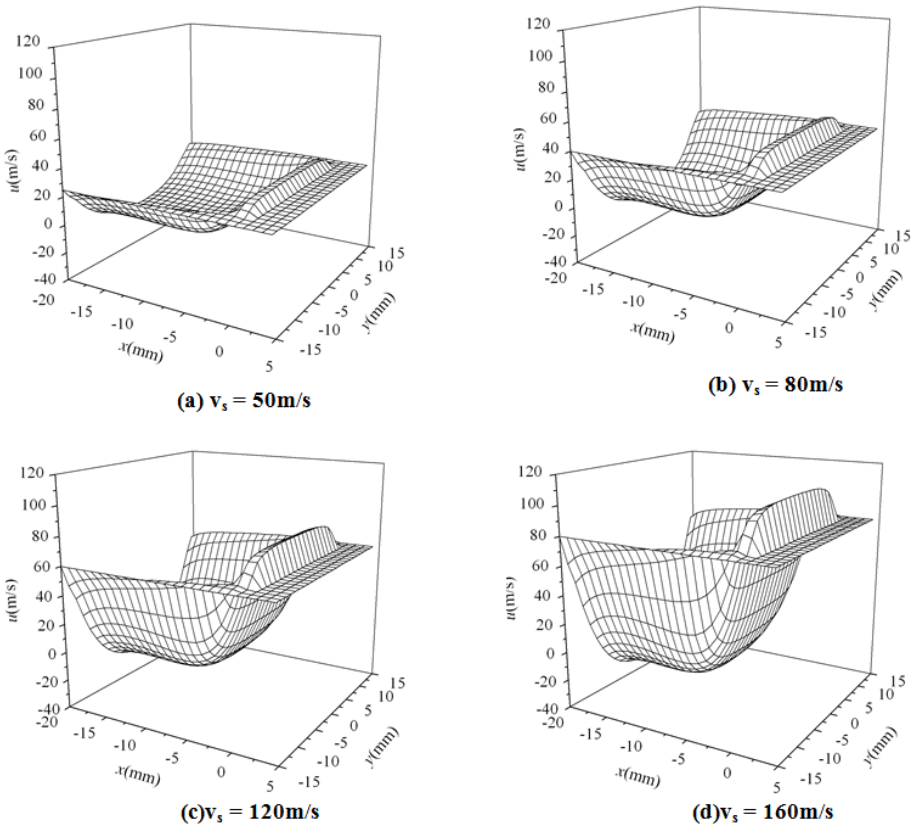

Figure 2. Fluid velocity distribution in direction x under different grinding wheel velocities

From Figure 2 and Figure 3, it can be seen that the velocity peak in direction x increased with the peripheral velocity of the grinding wheel. Around the minimum interval, the fluid velocity was the largest, and side discharge occurred along the width direction of the grinding wheel. The smaller the interval between the grinding wheel and workpiece (h_0) was, the greater the fluid velocity became, and the greater the velocity gradient of the fluid in direction x became. The negative velocity at the inlet was due to the existence of reflux, and the fluid velocity at the outlet almost remained fixed.

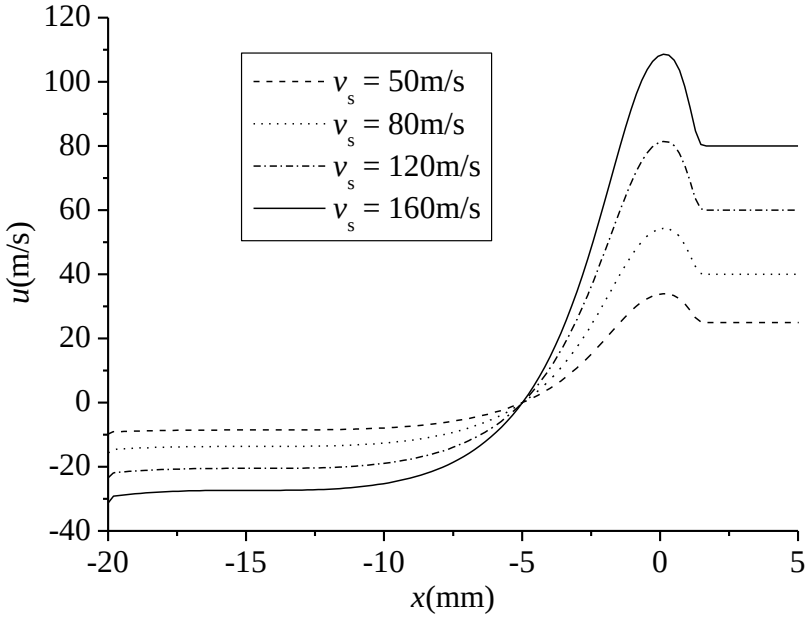

Figure 3. Variation curve of fluid velocity in direction x vs. peripheral velocity of grinding wheel

The grinding wheel has the diameter of 200mm, the width of 30mm and the peripheral velocity of 60m/s. The dynamic viscosity of grinding fluid is 0.05Pa s. With the above parameters being fixed, only the minimum interval between grinding wheel and workpiece was changed. The variation trend of the fluid velocity in the contact area in direction x was calculated, and the minimum interval h_0 was set at 30μm, 50μm, 80μm and 100μm in the calculation.

Figure 4 and Figure 5 show the variation trend of fluid velocity vs. minimum interval between grinding wheel and workpiece, from which it can be seen that the peak value of fluid velocity was basically free from the influence of minimum interval. Near the inlet, the minimum interval became smaller, and the variation gradient of velocity became larger; at the outlet, the fluid velocity basically remained unchanged.

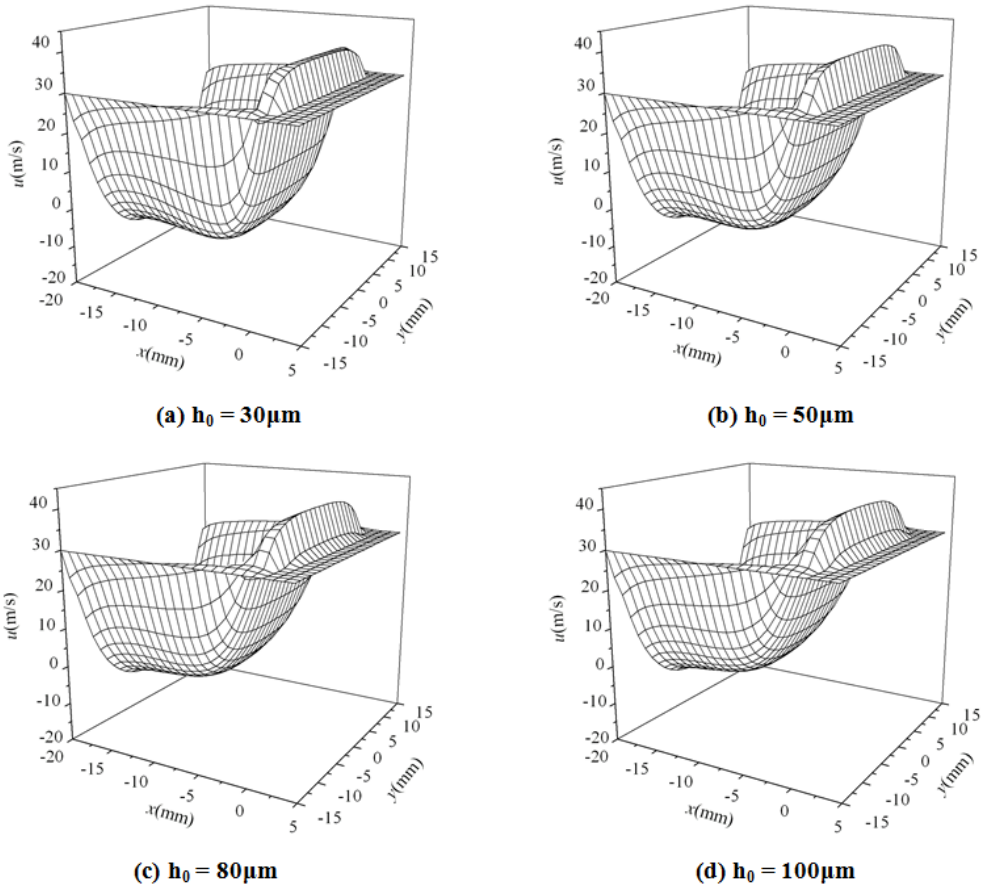

Figure 4. Fluid velocity distribution in direction x at different minimum intervals

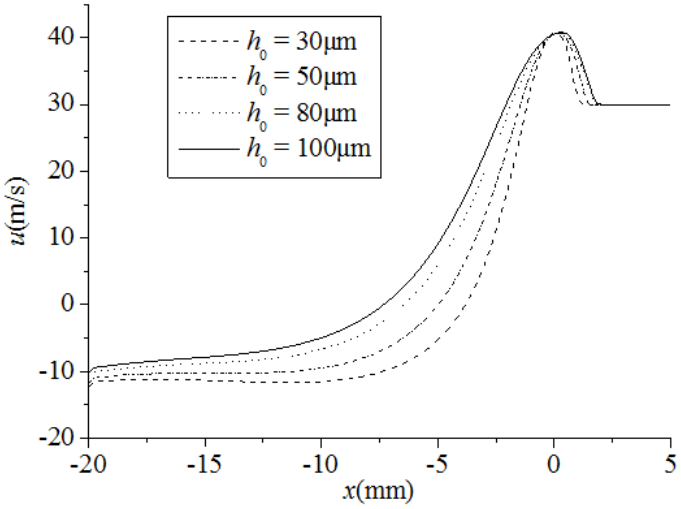

Figure 5. Variation curve of fluid velocity in direction x vs. minimum interval

3.2 The flow velocity changes along Y direction

The grinding wheel has the diameter of 200mm and the width of 30mm, the dynamic viscosity of grinding fluid is 0.05Pa s, and the minimum interval between the grinding wheel and a workpiece is h_0 = 50μm. With the above conditions remained fixed, only the peripheral velocity of the grinding wheel was changed. The variation trend of the fluid velocity in contact area in direction *y* was calculated, and the peripheral velocity of the grinding wheel was set at 50m/s, 80m/s, 120m/s and 160m/s in calculation.

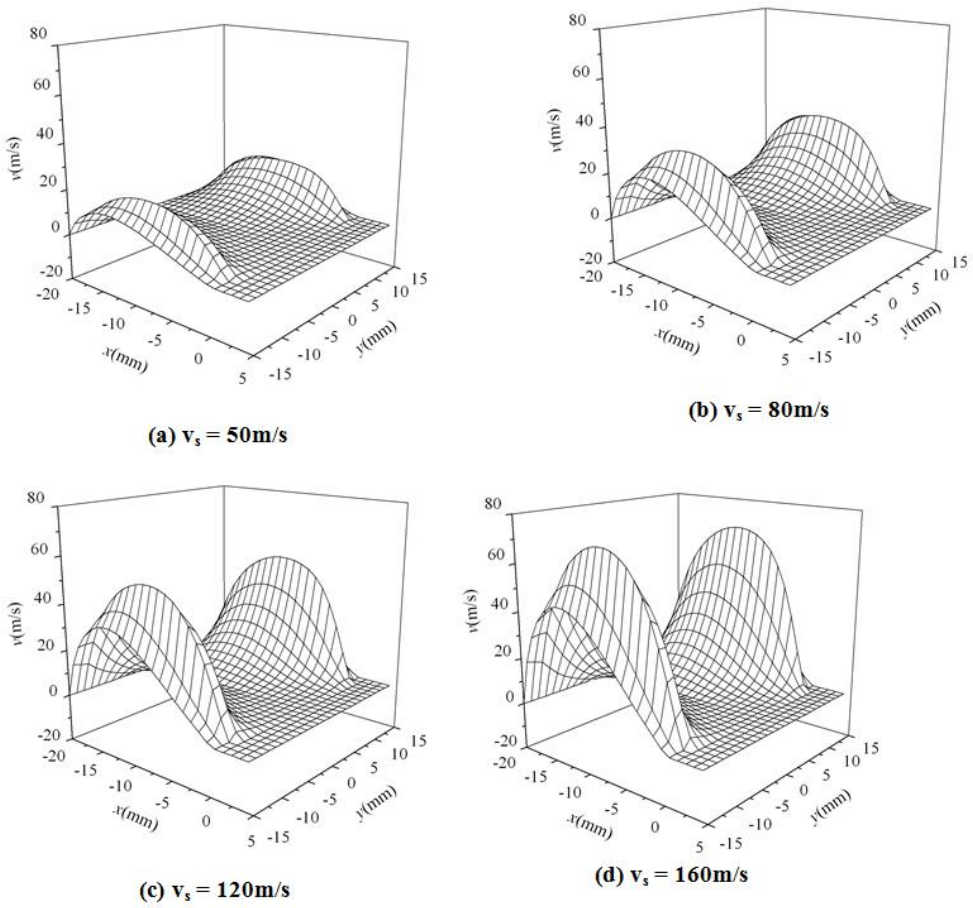

Figure 6. Fluid velocity distribution in direction y at different rotation velocities of grinding wheel

Figure 6 and Figure 7 show the fluid velocity distribution in direction *y* at different peripheral velocities of grinding wheel. The fluid velocity increased with increased peripheral velocity of grinding wheel. The fluid velocity at the edge of the grinding wheel along the width direction changed abruptly, because the dynamic pressure of the fluid produced side leakage at the wheel edge, which increased the fluid velocity. Except for the abrupt increase at the wheel edge, the fluid velocity in the width direction of the grinding wheel followed the same distribution law. Therefore, staggered network-like micro-insections are formed at the machining surface in the abrasive-flow jet precision finishing with grinding wheel as restraint, and the roughness and the waviness of the machining surface are reduced and made even.

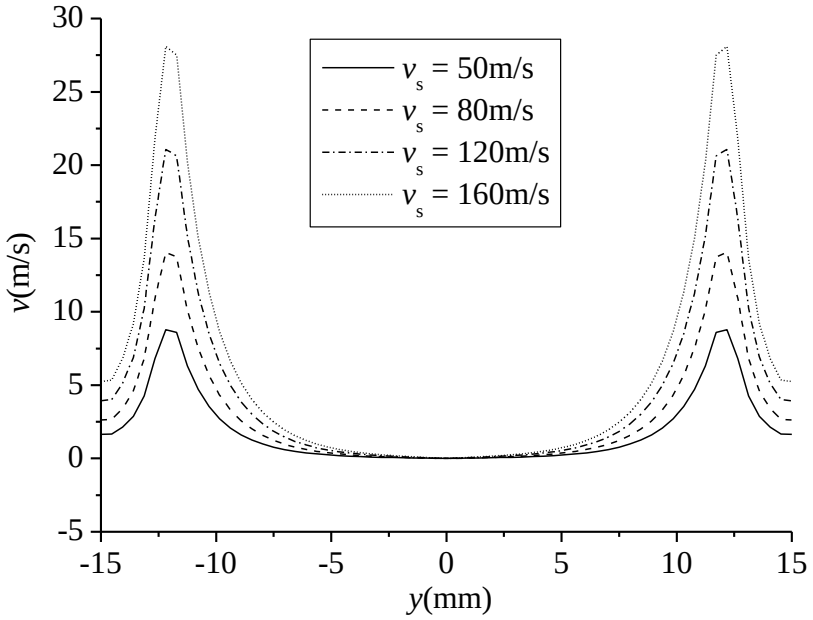

Figure 7. The velocity distribution of grinding fluid in direction y at different wheel velocity

Figure 8 shows the velocity distribution of grinding fluid in direction *y* at different minimum intervals, from which it can be seen that except for the fluid velocity at the width edge of the grinding wheel increased with the decrease of minimum interval, the velocity variation of grinding fluid in direction *y* basically kept fixed, indicating that the minimum interval between the grinding wheel and workpiece has slight impact on the velocity variation of grinding fluid in direction *y*.

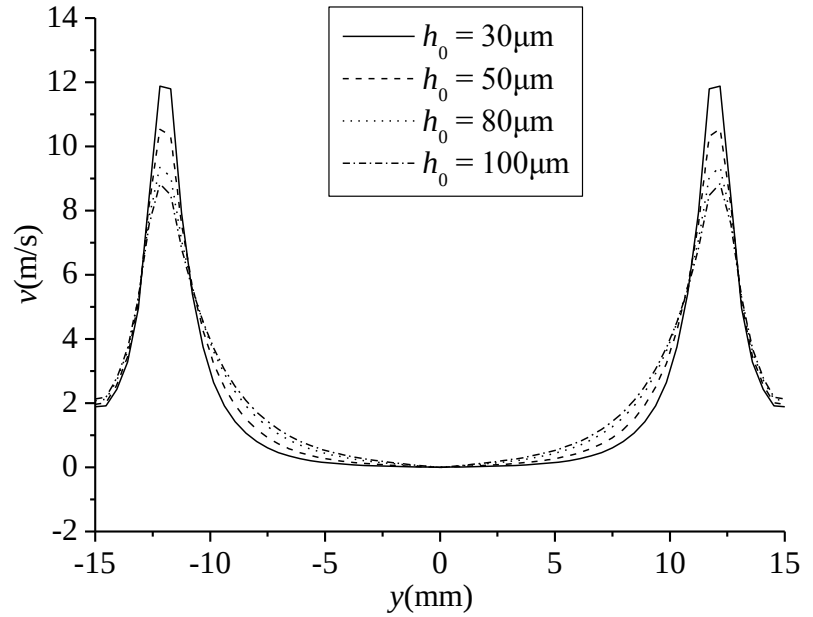

Figure 8. Variation curve of fluid velocity in direction y vs. minimum interval

3.3 Variation of fluid velocity in direction *z*

According to fluid lubrication theory, the velocity in the thickness direction of fluid, namely direction *z*, is zero and will not change with the peripheral velocity and the diameter of grinding wheel, nor with the minimum interval between grinding wheel and workpiece.

4. Experimental Results and Discussion

The experiments were conducted on the M7120 horizontal surface grinding machine, and the hot-wire anemometer was used to identify the velocity distribution patterns along the radial direction and width of the grinding wheel.

4.1 Flow field velocity distribution Patterns along the radial direction

Figure 9 shows the radial distribution of air flow field velocity along the radical direction of the grinding wheel (WA46J8V). It can be seen from Figure 9 that as the velocity increased, the velocity of the grinding wheel was also elevated. In addition, the closer to the surface, the greater the velocity will be.

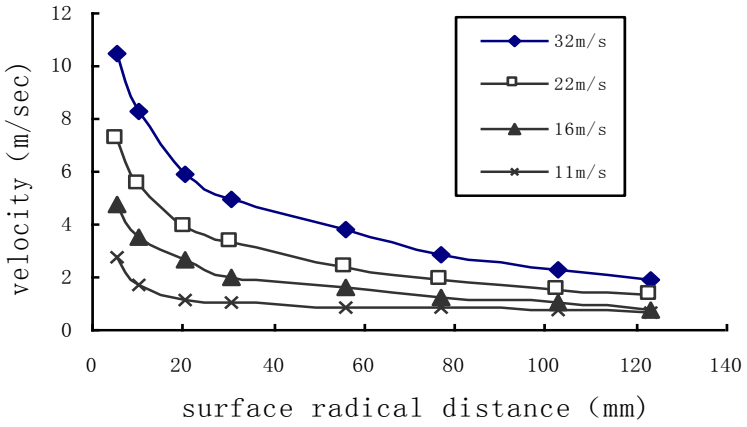

Figure 9. Radical Distribution of Airflow Field Velocity

With all the experimental conditions maintaining unchanged, we only replaced the wheel with the alumina wheel of the same shape. The experiment results were shown in Fig. 10. At the radical direction of the alumina wheel, the velocity dropped quickly. Yet, to a certain distance from the wheel, the velocity variation slowed down. It can be seen from the comparison between Figure 9 and Figure 10 that the velocity in the airflow field of the grinding wheel was much higher than that in the airflow field of the alumina wheel.

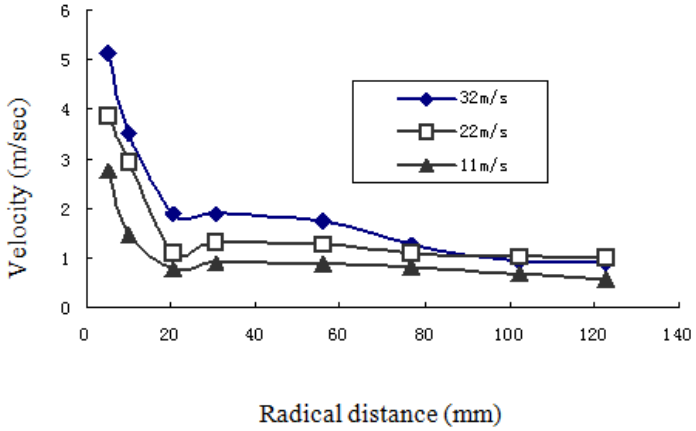

Figure 10. Radial Distribution of Airflow Field Velocity of Alumina Wheel

4.2 The Flow Field Velocity Distribution Patterns along the Wheel Width

The experiment was carried out at the peripheral velocity of 32m/s. The grinding wheel, coating wheel and solid aluminum wheel of the same shape were used for contrast tests, and the results are shown in Figure 11. It can be seen from the figure that ①two peak values at both sides of the grinding wheel along the width direction can be observed; ②as the porosity and the surface roughness increased, the velocity has been significantly increased.

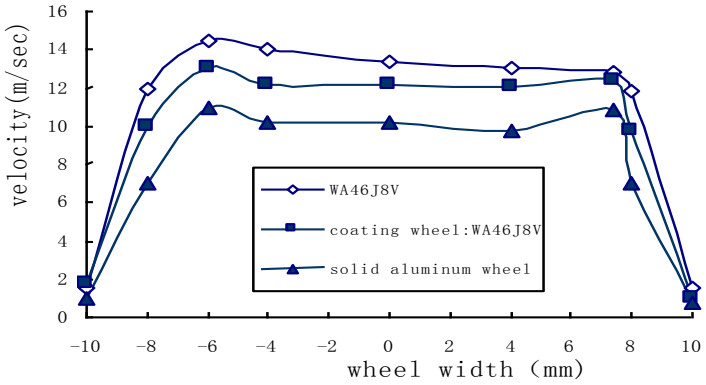

Figure 11. velocity distribution patterns of flow field along the width of the rotating wheel (peripheral velocity is 32m/s, 0.5mm from the wheel surface)

4.3 The impacts of air register on the radial velocity of flow field

It can be seen from Figure 12 that the air register can significantly reduce the velocity of the flow field so that the surface velocity dropped quickly, and then the velocity change became slowed down, tending to show almost no change. In addition, the smaller the included angle between the measuring points and the air register, the more obvious the change.

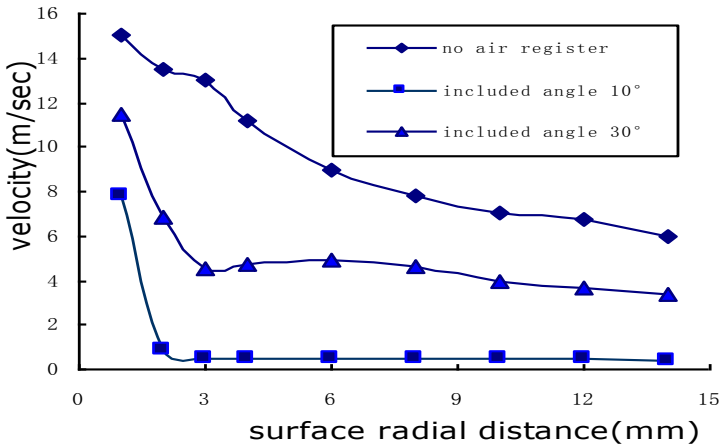

Figure 12. Impact of Air Register on Surface Airflow Field

5. Conclusion

On the basis of the analysis results, the following conclusions are drawn:

(1)According to Navier-Stokes equation and equation of continuity for fluid flow, the mathematical model of the wheel/workpiece wedge-shaped zone the velocity field was established.

(2)Simulation results of the velocity field in the wedge-shaped zone demonstrated that the flow velocity increased as the wheel velocity increased. The maximum peak velocity occurred in the minimum clearance area, and the gradient changes of the velocity in this area were significant; at the direction of wheel width, the distribution patterns of the flow velocity were the same, expect the rising at the verge of the wheel. At the inlet area, reflux occurred.

(3) The experiment research of the flow velocity field in the wedge-shaped area showed that the established model was consistent with the experimental results.

Acknowledgements

This research was financially supported by the National Natural Science Foundation of China (50875138; 51175276), the Shandong Provincial Natural Science Foundation of China (Z2008F11; ZR2009FZ007).

References

[1] S. Ebbrell, N. H. Woolley, Y. D. Tridimas, D. R. Allanson and W. B. Rowe, "The effects of cutting fluid application methods on the grinding process", International Journal of Machine Tools & Manufacture, vol. 40, no. 2, **(2000)**, pp. 209–223.
[2] C. Guo and S. Malkin, "Analysis of fluid flow through the grinding zone", Journal of Engineering for Industry, vol. 114, no. 4, **(1992)**, pp. 427-434.
[3] C. Guo and S. Malkin, "Experimental measurement of fluid flow through the grinding zone", Journal of Engineering for Industry, vol. 114, no. 1, **(1992)**, pp. 61-66.
[4] Y. Saito, N. Nishiwaki and Y. Ito, "An Investigation of Local Heat Transfer During Grinding Process--Effects of Porosity of Grinding Wheel", American Society of Mechanical Engineers, vol. 101, no. 5, **(1978)**, pp. 97-103.
[5] J. Shibata, T. Goto, M. Yamamoto, *et al.*, "Characteristics of air flow around a grinding wheel and their availability for assessing the wheel wear", CIRP Annals-Manufacturing Technology, vol. 31, no. 1, **(1982)**, pp. 233-238.

[6] J. F. Rahman and V. Radhakrishnan, "Surface condition monitoring of grinding wheels by pneumatic back-pressure measurement", Wear, vol. 70, no. 2, **(1981)**, pp. 219-226.
[7] V. Radhakrishnan and J. F. Rahman, "Functional assessment of the grinding wheel surface characteristics by turbulence amplifier", J. Eng. Ind., vol. 103, no. 1, **(1981)**, pp. 99-102.
[8] M. N. Morgan, A. R. Jackson and H. Wu, "Optimisation of fluid application in grinding", CIRP Annals-Manufacturing Technology, vol. 57, no. 1, **(2008)**, pp. 363-366.
[9] N. Patir and H. S. Cheng, "An Average Flow Model for Determining Effects of Three-Dimensional Roughness on Partial Hydrodynamic Lubrication", ASME J. Lubr. Technol., vol. 100, **(1978)**, pp. 12–17.
[10] C. H. Li, Y. L. Hou, Z. Fang, *et al.*, "Analytical and experimental investigation of grinding fluid hydrodynamic pressure at wedge-shaped zone", International Journal of Abrasive Technology, vol. 4, no. 2, **(2011)**, pp. 140-155.
[11] E. Brinksmeier and E. Minke, "High-performance surface grinding— the influence of coolant on the coolant process", Annals of the CIRP, vol. 42, no. 1, **(1993)**, pp. 367–370.
[12] C. C. Chang, "An application of lubrication theory to predict useful flow-rate of coolant on grinding porous media", Tribology international, vol. 30, no. 8, **(1997)**, pp. 575-581.
[13] C. Frank, Z. Wojciech and F. Edwin, "Fluid Performance Study for Groove Grinding a Nickel-Based Superalloy Using Electroplated Cubic Boron Nitride (CBN) Grinding Wheels", Journal of Manufacturing Science and Engineering, vol. 126, no. 3, **(2004)**, pp. 451-458.
[14] F. Katsushi, O. Noriyuki, H. N. Trong and T. Nakamura, "In-process measurement of topography change of grinding wheel by using hydrodynamic pressure", International Journal of Machine Tools & Manufacture, vol. 42, no. 13, **(2002)**, pp. 1447–1453.
[15] Y. L. Hou, C. H. Li and Q. Zhang, "Investigation of structural parameters of high speed grinder spindle system on dynamic performance", Int. J. Materials and Product Technology, vol. 44, no. 1/2, **(2012)**, pp. 92-114.
[16] C. H. Li, Y. L. Hou, Y. C. Ding and G. Q. Cai, "Feasibility investigations on compound process: a novel fabrication method for finishing with grinding wheel as restraint", International Journal of Computational Materials Science and Surface Engineering, vol. 4, no. 1, **(2011)**, pp. 55 - 68.
[17] V. K. Gviniashvili, N. H. Woolley and W. B. Rowe, "Useful coolant flowrate in grinding", International Journal of Machine Tools & Manufacture, vol. 44, no. 6, **(2004)**, pp. 629-636.
[18] C. H. Li, Y. L. Hou, Z. R. Liu and Y. C. Ding, "Investigation into temperature field of nano-zirconia ceramics precision grinding", International Journal of Abrasive Technology, vol. 4, no. 1, **(2011)**, pp. 77-89.
[19] V. Gviniashvili, J. Webster and B. Rowe, "Fluid Flow and Pressure in the Grinding Wheel-Workpiece Interface", Transactions of the ASME, vol. 127, no. 1, **(2005)**, pp. 198-205.
[20] P. Hryniewicz, A. Z. Szeri and S. Jahanmir, "Application of Lubrication Theory to Fluid Flow in Grinding: Part I-Flow Between Smooth Surfaces", Journal of Tribology ASME, vol. 123, no. 1, **(2001)**, pp. 94–100.
[21] H. Yali, L. Changhe, H. Zhenlu, *et al.*, "Examination of the Material Removal Mechanisms During the Abrasive Jet Finishing of 45 Steel", Adv. Sci. Lett., vol. 4, no. 4-5, **(2011)**, pp. 1478-1484.
[22] Y. Hou, C. Li and Y. Zhou, "Applications of High-Efficiency Abrasive Process with CBN Grinding Wheel", Engineering, vol. 2, no. 3, **(2010)**, pp. 184-189.
[23] F. Klocke, A. Baus and T. Beck, "Coolant induced forces in CBN high speed grinding with shoe nozzle", Annals of the CIRP, vol. 49, no. 1, **(2000)**, pp. 241-244.
[24] L. Sun-Kyu, M. Yuji, K. Tsunemoto and S. Katsuo, "Effects of minimizing hydrodynamic pressure in ultra-precision mirror grinding", International Journal of Machine Tools & Manufacture, vol. 44, no. 10, **(2004)**, pp. 1031–1036.
[25] C. H. Li, G. Q. Cai and S. C. Xiu, "Hydrodynamic Pressure Modeling and Verification of Contact Zone on Abrasive Jet Finishing with Grinding Wheel as Restraint", Acta Armamentarii, vol. 28, no. 2, **(2007)**, pp. 202-205.
[26] S. Wang, C. H. Li and Y. C. Ding, "Investigation into Speed and Temperature Field of Metal Drop in High-melting Metal Arc Spraying", International Journal of Control and Automation, vol. 5, no. 3, **(2012)**, pp. 237-248.
[27] B. Zhang and A. Nakajima, "Hydrodynamic Fluid Pressure in Grinding Zone During Grinding With Metal-Bonded Diamond Wheels", Journal of Tribology, vol. 122, no. 2, **(2000)**, pp. 603-608.
[28] W. Sheng and L. Changhe, "Application and Development of High-efficiency abrasive process", International Journal of Advanced Science and Technology, vol. 47, no. 10, **(2012)**, pp. 51-64.
[29] Z. L. Han and C. H. Li, "Theoretical Modeling and Simulation of Airflow Field near Grinding Wheel", International Journal of Control and Automation, vol. 6, no. 4, **(2013)**, pp. 145-155.

